

Generation of Laguerre–Gaussian modes in fiber-coupled laser diode end-pumped lasers

Y.F. Chen^{1,*}, Y.P. Lan², S.C. Wang²

¹Department of Electrophysics, National Chiao Tung University, Hsinchu, Taiwan, Republic of China

²Institute of Electro-Optical Engineering, National Chiao Tung University, Hsinchu, Taiwan, Republic of China

Received: 8 June 2000/Revised version: 2 July 2000/Published online: 20 September 2000 – © Springer-Verlag 2000

Abstract. A technique has been developed for the generation of Laguerre–Gaussian ($LG_{0,l}$) modes in a fiber-coupled laser diode end-pumped microchip laser. A theoretical model is also developed to predict how the oscillation of $LG_{0,l}$ modes is affected by the pump position, the pump size and the cavity mode size. With a 1-W fiber-coupled diode, the highest-order $LG_{0,l}$ mode that can be generated is $l = 23$.

PACS: 42.55; 42.60

The high-order Laguerre–Gaussian ($LG_{p,l}$) mode exhibits interesting physics and has the potential for technological applications [1–4], where p and l are the radial and azimuthal indices of the LG mode. A pure high-order $LG_{0,l}$ -mode has been reported in electrically pumped [5, 6] and optically pumped [7] vertical-cavity surface-emitting semiconductor lasers (VCSELs). However, the main difficulty of the emission of high-order LG modes in VCSELs is that the processed wafer is in need of extraordinary homogeneity.

Diode-pumped solid-state lasers offer the advantages of high efficiency, compactness and reliability, especially in an end-pumping configuration [8]. Fiber delivery of the pump power enables us to keep the laser resonator apart from the pump source, so that the laser resonator can be isolated from disturbances of the pump source [9]. Recently, we have generated high-order Hermite–Gaussian modes by a fiber-coupled diode end-pumped Nd:YAG laser [10, 11]. In this letter, we report a technique for the generation of the pure LG modes with $p = 0$ and specified values of l in a fiber-coupled diode end-pumped microchip laser. The key novelty is to produce a doughnut-shaped pump profile by defocusing a standard fiber-coupled diode. We also develop a theoretical model to analyze how the focal position of the pump beam in the laser crystal influences the oscillation of $LG_{0,l}$ modes. Experimental results have shown a fairly good agreement with theoretical predictions.

*Corresponding author.

(Fax: +866-35/729-134, E-mail: yfchen@cc.nctu.edu.tw)

For a multi-mode fiber-coupled diode laser beam passing through a focusing lens, the profile at the focal plane is like a top-hat distribution; however, away from the focal plane it is like a doughnut-shaped distribution, as shown in Fig. 1a. With this property, we can defocus a standard fiber-coupled diode to result in a good overlap with the high-order $LG_{0,l}$ mode and generate it purely. Figure 1b shows the schematic of a fiber-coupled laser diode end-pumped Nd:YVO₄ laser considered in this work. In our experiments, we have used a plano-concave cavity that consists of one planar Nd:YVO₄ surface, high-reflection coated at 1064 nm and high-transmission coated at 809 nm for the pump light to enter the laser crystal, and a spherical output mirror. The second surface of the Nd:YVO₄ crystal (1-mm length) is anti-reflection-coated at 1064 nm. A mirror with a reflectance

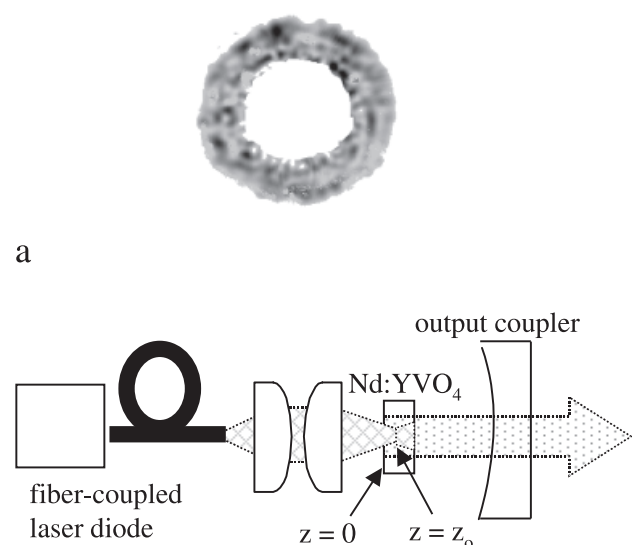


Fig. 1. **a** A typical beam profile of a fiber-coupled laser diode away from the focal plane. **b** Schematic of a fiber-coupled diode end-pumped solid-state laser

of $R = 98.5\%$ and a radius of curvature of 25 cm was used in the resonator to couple the output power. For a 1-cm resonator length, the waist of the fundamental mode was around 0.24 mm. The fiber-coupled laser diode (Coherent, F-81-800C-100) has a 0.1-mm core diameter and was focused into the Nd:YVO₄ crystal by using a focusing lens with 0.57 magnification.

Figure 2 shows a sketch of the position dependence of the beam profile for a multi-mode fiber-coupled laser-diode beam passing through a focusing lens. According to the property of the beam profile, the normalized pumping distribution in the laser crystal is approximated as

$$R_p(r, z) = \frac{1}{\pi\omega_p^2} \frac{\alpha e^{-\alpha z}}{1 - e^{-\alpha L}} \Theta(r - \theta_p |z - z_0|) \times \Theta\left(\sqrt{(\theta_p(z - z_0))^2 + \omega_p^2} - r\right), \quad (1)$$

where ω_p is the radius at the waist, α is the absorption coefficient at the pump wavelength, L is the length of the laser crystal, θ_p is the far-field half-angle, the point $z = 0$ is taken to be at the incident surface of the gain medium, z_0 is the focal position of the pump beam in the laser crystal and $\Theta()$ is the Heaviside step function. The functional form of (1) comes from the fact that the pump profile is like a top-hat distribution at the focal plane and like a ring-type distribution away from the focal plane.

The expected preferred laser modes in the ring shape of the pump beam are the LG_{0,l} modes, since these show optimum overlap with the ring pump. For an end-pumped solid-state laser, the threshold pump power for a single LG_{0,l} mode oscillation is given by [10]

$$P_{\text{th},0,l} = \frac{\gamma I_{\text{sat}}}{\eta_p L} \frac{1}{\int \int s_{0,l}(r, \phi, z) R_p(r, z) dV}, \quad (2)$$

where γ is the total logarithmic loss per pass, I_{sat} is the saturation intensity, L is the length of the active medium, and $\eta_p = \eta_t \eta_a (v_l/v_p)$ where η_t is the optical transfer efficiency (ratio between optical power incident on the active medium and that emitted by the pump source), η_a is the absorption efficiency (ratio between power absorbed in the active medium and that entering the rod) and v_p and v_l are pump and laser frequencies, respectively. $s_{0,l}(r, \phi, z)$ is the normalized cavity mode intensity distribution. Equation (2) indicates that the LG_{0,l} mode with the biggest overlap with the gain structure has the minimum threshold and will dominate in the laser output.

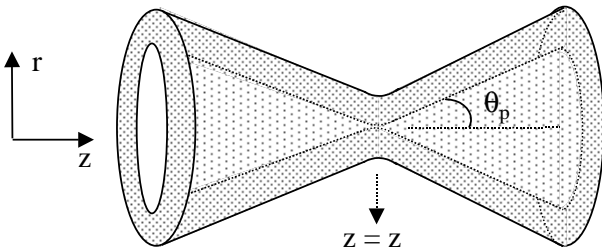


Fig. 2. A sketch of the position dependence of the beam profile for a multi-mode fiber-coupled laser-diode beam passing through a focusing lens

Considering a single LG_{0,l} mode, $s_{0,l}(r, \phi, z)$ is given by

$$s_{0,l}(r, \phi, z) = \frac{4}{(1 + \delta_{0,l})l!} \frac{1}{\pi\omega_0^2 L} \times (\cos^2 l\phi) \left(\frac{2r^2}{\omega_0^2}\right)^l \exp\left(-\frac{2r^2}{\omega_0^2}\right), \quad (3)$$

where the z -dependent variation in $s_{0,l}(r, \phi, z)$ is neglected and the spot radius of the laser beam ω_0 is approximated to be constant along the laser axis in the laser crystal.

Substituting (1) and (3) into (2) and carrying out the integrations over r and ϕ , we obtain

$$P_{\text{th},0,l}(z_0) = \frac{\pi\gamma I_{\text{sat}}}{\eta_p} \frac{1 - e^{-\alpha L}}{\alpha} \frac{\omega_p^2}{L \int_0^L Q_l(z_0) \exp(-\alpha z) dz}, \quad (4)$$

where

$$Q_l(z_0) = \sum_{j=0}^l \frac{1}{(l-j)!} \times \left\{ e^{l-j} \exp(-\varrho) - \left(\varrho + \frac{2\omega_p^2}{\omega_0^2}\right)^{l-j} \exp\left[-\left(\varrho + \frac{2\omega_p^2}{\omega_0^2}\right)\right] \right\}, \quad (5)$$

and

$$\varrho = 2 \left[\frac{\theta_p(z - z_0)}{\omega_0} \right]^2. \quad (6)$$

With the parameters of the present cavity: $\omega_0 = 0.24$ mm, $\omega_p = 0.028$ mm, $\theta_p = 0.34$ rad, $\gamma = 0.016$, $\eta_p = 0.8$, $L = 1$ mm, $I_{\text{sat}} = 13.87$ W/mm² and $\alpha = 3$ mm⁻¹, the threshold power for different LG_{0,l} modes was calculated as a function of the focal position of the pump beam in the laser crystal. Figure 3 shows the dependence of the threshold power on the focal position of the pump beam for the first six LG_{0,l} modes. The results show that the LG_{0,0} mode has the minimum threshold power for the focal position in the range between $z_0 = -0.3$ and $z_0 = 1.0$. Farther away from the superior range of the LG_{0,0} mode, the higher-order LG_{0,l} mode has the minimum threshold power. This result indicates that adjusting the focal position of the pump beam can lead to the generation of the LG_{0,l} modes with specified values of l . Since the transverse mode with the minimum threshold power can break into oscillation at first, the dependence of the threshold power on the focal position is given by $P_{\text{th},\min}(z_0) = \min\{P_{\text{th},0,l}(z_0)\}$.

Experimental results for the threshold power versus the focal position of the pump beam z_0 are shown in Fig. 4. It can be seen that experimental data agree very well with the calculations of the theoretical analysis. Figure 5 shows the beam profiles with different LG_{0,l}-mode distributions, measured with the CCD camera (Coherent, Beam-Code), in the fourteen positions. The relationship between the dominant LG_{0,l} mode and the focal position of the pump beam is also consistent with the theoretical predictions as shown in Fig. 4. In our experiment, the highest-order LG_{0,l} mode that can be obtained with a 1-W fiber-coupled diode is $l = 23$, as shown

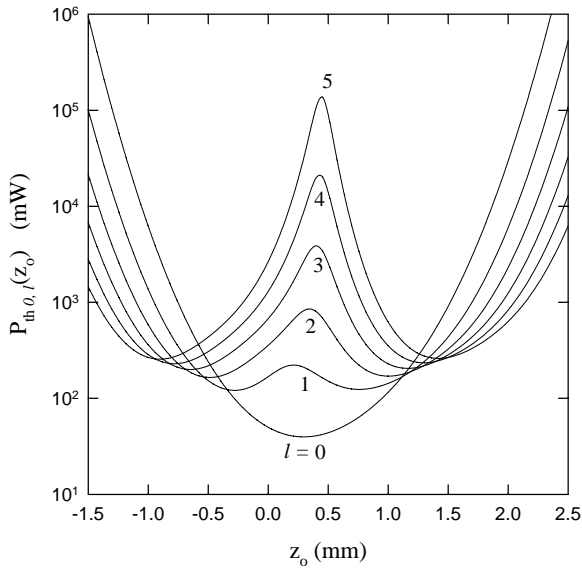


Fig. 3. The dependence of the threshold power on the focal position of the pump beam for the first six $LG_{0,l}$ modes

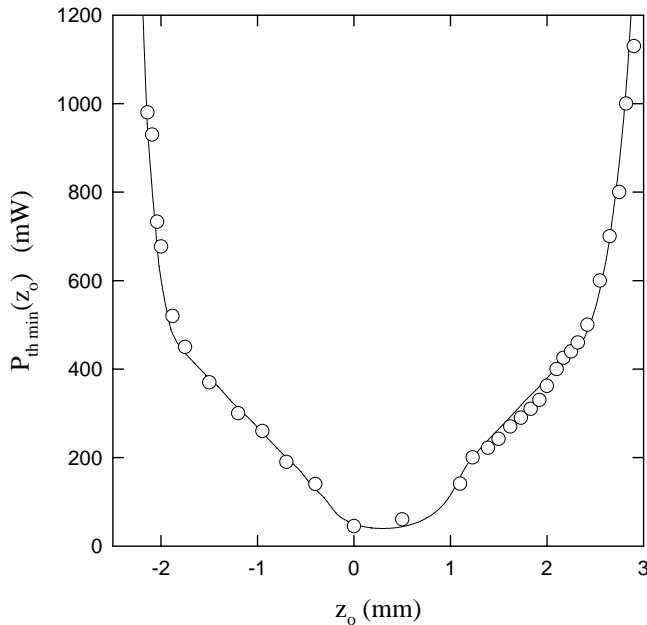


Fig. 4. A plot of experimental results (symbols) and theoretical results (solid line) of the threshold power versus the focal position of the pump beam z_0

in Fig. 6. It is worth mentioning that the present analysis does not take saturation effects into account. Saturation of gain by the first mode to reach threshold can raise the threshold of the other modes by a factor of about $1.2 \sim 2$. Experimental results show that the times-above-threshold factor before additional modes to oscillate depends on the mode number, i.e. the diameter of the pumping doughnut. A theoretical model for the saturation effect is currently under way.

We have generated the pure $LG_{0,l}$ modes in an end-pumped microchip laser by defocusing a standard fiber-coupled diode to produce a doughnut-shaped pump profile. A theoretical analysis has also been provided to calculate the threshold pump power of $LG_{0,l}$ modes as a function of the

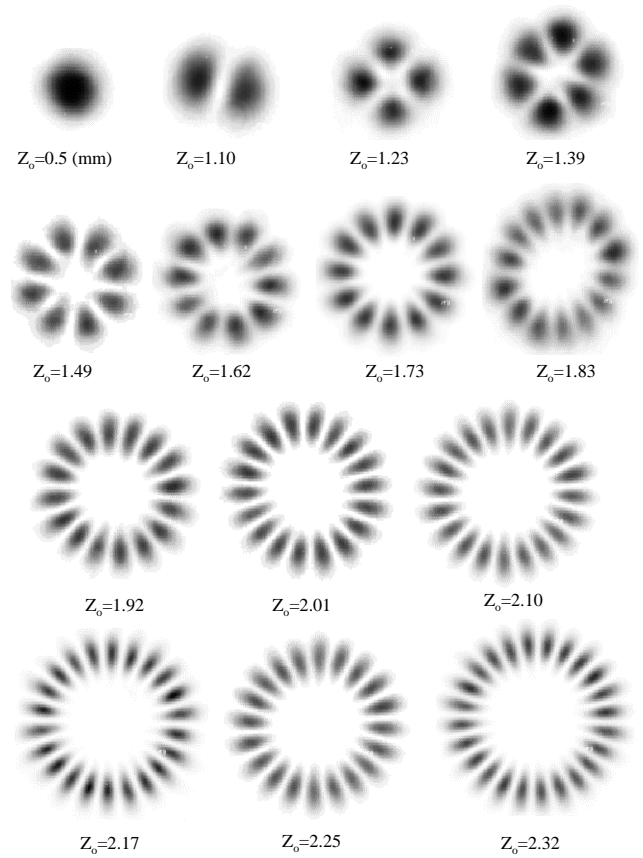


Fig. 5. Beam profiles with different $LG_{0,l}$ -mode distributions, measured with the CCD camera, in the fourteen positions

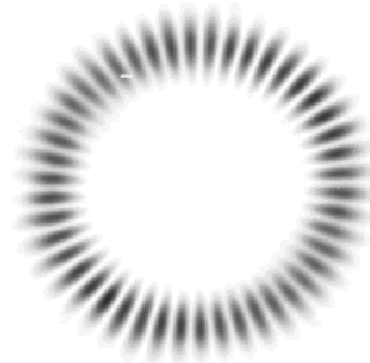


Fig. 6. The beam profile of the highest-order $LG_{0,l}$ mode with $l = 23$

laser-diode beam quality, the focal position of the pump beam and the cavity parameters. Experimental results have shown a fairly good agreement with the predictions of the present analysis.

References

1. S.L. McCall, A.F.J. Levi, R.E. Slusher, S.J. Pearton, R.A. Logan: Appl. Phys. Lett. **60**, 289 (1992)
2. D.Y. Chu, M.K. Chin, W.G. Bi, H.Q. Hou, C.W. Tu, S.T. Ho: Appl. Phys. Lett. **65**, 3167 (1994)
3. M.J. Ries, E.I. Chen, N. Holonyak Jr.: Appl. Phys. Lett. **68**, 2035 (1996)

4. L. Dijaloshinski, M. Orenstein: *Opt. Lett.* **23**, 364 (1998)
5. C. Degen, I. Fischer, W. Elsässer: *Opt. Exp.* **5**, 38 (1999)
6. Q. Deng, H. Deng, D.G. Deppe: *Opt. Lett.* **22**, 463 (1997)
7. S.F. Pereira, M.B. Willemsen, M.P. van Exter, J.P. Woerdman: *Appl. Phys. Lett.* **73**, 2239 (1998)
8. J. Berger, D.F. Welch, D.R. Scifres, W. Streifer, P. Cross: *Appl. Phys. Lett.* **51**, 1212 (1987); D.L. Sipes: *Appl. Phys. Lett.* **47**, 74 (1985)
9. H. Hemmati, J.R. Lesh: *Opt. Lett.* **19**, 1322 (1994); Y. Kaneda, M. Oka, H. Masuda, S. Kubota: *Opt. Lett.* **17**, 1003 (1992); J. Berger, D.F. Welch, W. Streifer, D.R. Scifres, N.J. Hoffman, J.J. Smith, D. Radecki: *Opt. Lett.* **13**, 306 (1988)
10. Y.F. Chen, T.M. Huang, C.F. Kao, C.L. Wang, S.C. Wang: *IEEE J. Quantum Electron.* **QE-33**, 1025 (1997)
11. H. Laabs, B. Ozygus: *Opt. Laser Technol.* **28**, 213 (1996)